

Observation of p-wave Threshold Law Using Evaporatively Cooled Fermionic Atoms

B. DeMarco, J. L. Bohn, J. P. Burke, Jr., M. Holland, and D. S. Jin*

JILA,

National Institute of Standards and Technology and University of Colorado,
and

Physics Department, University of Colorado, Boulder, CO 80309-0440

(August 16, 2021)

We have measured independently both s-wave and p-wave cross-dimensional thermalization rates for ultracold ^{40}K atoms held in a magnetic trap. These measurements reveal that this fermionic isotope has a large positive s-wave triplet scattering length in addition to a low temperature p-wave shape resonance. We have observed directly the p-wave threshold law which, combined with the Fermi statistics, dramatically suppresses elastic collision rates at low temperatures. In addition, we present initial evaporative cooling results that make possible these collision measurements and are a precursor to achieving quantum degeneracy in this neutral, low-density Fermi system.

While many examples of quantum degenerate fermionic systems are found in nature (electrons in metals and nucleons in nuclear matter, for example), low density Fermi systems are exceedingly rare. However, techniques similar to those that led to the observation of Bose-Einstein condensation (BEC) in atomic systems [1] can be exploited to realize a quantum degenerate, dilute gas of fermionic atoms. Novel phenomena predicted for this system include the suppression of inelastic collisions [2], linewidth narrowing through suppression of spontaneous emission [3], and the possibility of a phase transition to a superfluid-like state at sufficiently low temperatures [4]. Just as was found in the case of BEC in alkali atoms, knowledge of the binary elastic collision cross-sections and interatomic potentials is crucial for experiments on fermionic species. Both evaporative cooling and the prospect of fermionic superfluidity depend on the cold collision parameters. For example, accurate prediction of magnetic-field Feshbach resonances [5], which could be used to realize Cooper pairing of fermionic atoms, hinges on detailed understanding of the interatomic potentials. In this letter, we present measurements of elastic collision cross sections for evaporatively cooled ^{40}K , including a direct observation of p-wave threshold behavior and the resultant strong suppression of the collision rate.

Among the stable fermionic alkali atoms, ^{40}K yields the greatest range of possibilities for evaporative cooling strategies and interaction studies because of its large atomic spin, F ($F=9/2$ and $F=7/2$ hyperfine ground states). In addition to having a large number of spin states that can be held in the usual magnetic traps,

potassium has two bosonic isotopes, ^{39}K and ^{41}K , which could be used for future studies of mixed boson-fermion dilute gases. Forced evaporative cooling [6], which has proven essential for achieving quantum degeneracy in bosonic alkali gases, relies on elastic collisions for rethermalization of the trapped atomic gas. However, evaporative cooling strategies for fermionic samples are complicated by the fact that atomic collisions at these low temperatures (100's of μK and below) are predominantly s-wave in character for bosonic atoms, while the Pauli exclusion principle prohibits s-wave collisions between spin-polarized fermions. Evaporative cooling for fermionic atoms must then proceed either through p-wave collisions [7] or through sympathetic cooling [8].

Since the s-wave and p-wave binary elastic cross sections are not well known for ^{40}K [9–11], we have made measurements of elastic collision rates in a magnetic trap. The Fermi-Dirac quantum statistics of ^{40}K provide a unique opportunity to observe p-wave collisions directly. Exploiting this fact, we have seen evidence for a p-wave shape resonance and have observed threshold behavior of the p-wave cross section. To our knowledge, this measurement represents the first direct verification of the p-wave threshold law for neutral scatterers.

We use a double-MOT (magneto-optical trap) apparatus [12] to trap and pre-cool ^{40}K atoms prior to loading them into a purely magnetic trap. Operation of the MOT's employs two MOPA (master-oscillator power-amplifier) diode laser systems [13], each frequency stabilized using the DAVLL (dichroic absorption vapor laser lock) technique [14] which accomplishes a large frequency range for locking. Also, we have developed an atom source [15] that is enriched with 5% ^{40}K (whose natural abundance is 0.01%). This system allows us to trap any of the three potassium isotopes, and to trap 10^8 ^{40}K atoms (four orders of magnitude more ^{40}K atoms than previous efforts [16]).

Immediately before loading the sample into the magnetic trap, the atoms are cooled to approximately $150 \mu\text{K}$ during a Doppler cooling stage of the MOT in which the trapping light is jumped closer to resonance. Further, an optical pumping pulse transfers the majority of the atoms into magnetically trappable states in the $F=9/2$ hyperfine ground state. The atoms are then loaded into a cloverleaf magnetic trap [17] and after an initial evaporative cooling stage, we are left with roughly 10^7 ^{40}K

atoms at 60 μK and a peak density of 10^9 cm^{-3} . The cloverleaf magnetic trap provides a cylindrically symmetric harmonic potential, with a characteristic radial frequency $\nu_r = 44 \pm 1$ and an axial frequency ν_z of 19 ± 1 Hz for loading. The lifetime of the atoms in the magnetic trap, limited by collisions with room-temperature background atoms, has an exponential time constant of 300 ± 50 s, giving ample time for thermal relaxation studies as well as for evaporation. The radial frequency and the bias magnetic field can be altered smoothly by changing the current through a pair of Helmholtz bias coils.

We determine elastic collision cross sections from measurements of cross-dimensional thermalization rates [18] in the magnetic trap. The sample is taken out of thermal equilibrium by changing ν_r through a ramp of the bias coil current. For the measurements reported here ν_r lies between 44 and 133 Hz. The change in ν_r occurs adiabatically (slow compared to the atomic motion in the trap) but much faster than the rate of collisions between atoms. Since the axial frequency is essentially unchanged, energy is added to (or removed from) the cloud in only the radial dimension. Elastic collisions then move energy between the radial and the axial dimensions, and the thermal relaxation is observed by monitoring the time evolution of the cloud's aspect ratio.

To avoid perturbations to the image due to the spatially dependent magnetic fields, the trap is turned off suddenly and the cloud is imaged after 2.7 ms of free expansion. The aspect ratio of the cloud is observed via absorption imaging using a 9.1 μs pulse of light resonant with the $4S_{1/2}, F=9/2$ to $4P_{3/2}, F=11/2$ transition. Optical depth is calculated from the image captured on a CCD array and then surface fit to a gaussian distribution to find the rms cloud size in both the radial and axial dimensions. An example of the cloud evolution following a change in trap potential is shown in Fig. 1. Since the expanded cloud sizes are proportional to the square root of the cloud energy in each dimension, the exponential time constant for the redistribution of energy, τ , can be extracted from an appropriate fit to the aspect ratio vs time. To rule out significant relaxation through trap anharmonicities, we have verified that the relaxation rate $1/\tau$ scales linearly with the number of trapped atoms N .

To obtain the elastic collision cross section σ from our measurements of thermal relaxation rates, we use the relation: $1/\tau = \frac{2}{\alpha} n \sigma v$, where n is the density-weighted density of the trapped atoms given by $\frac{1}{N} \int n(r)^2 d^3r$, v is the rms relative velocity between two atoms in the trap, and α is the calculated average number of binary collisions per atom required for thermalization. The product $n v$ depends on both the size and temperature, T , of the trapped sample. These are measured by observing the expansion of an equilibrated sample after release from the magnetic trap. The rate of expansion yields the temperature, while an extrapolation back to the release time gives the initial sizes. Using the trap potential calculated

from the field coil geometry we have checked that the measured initial sizes and temperatures are consistent to within their uncertainties.

The mean number of collisions each atom undergoes, α , during one relaxation time constant was determined from a numerical simulation of the experiment using classical Monte Carlo methods [19]. For a harmonic trapping potential, the relaxation simulation yields $\alpha_s = 2.5$ for s-wave collisions and $\alpha_p = 4.1$ for p-wave collisions. The ratio α_p/α_s can also be determined analytically through an integration over the angular dependence of scattering. This gives $\alpha_p/\alpha_s = 5/3$, consistent with the Monte Carlo results.

The primary results of this paper are shown in Fig. 2. While ordinarily one cannot measure higher order partial wave contributions to the collision cross section directly, the Fermi-Dirac statistics of ^{40}K allow us to probe p-wave and s-wave interactions independently. The p-wave cross section σ_p is determined from measurements using a spin-polarized sample ($|F = 9/2, m_F = 9/2 \rangle$ atoms), where s-wave collisions are prohibited by the quantum statistics. The s-wave cross sections σ_s are determined from data obtained using a mixture of two spin states, $|9/2, 9/2 \rangle$ and $|9/2, 7/2 \rangle$. The magnitude of the p-wave cross section is surprisingly large and we find that ^{40}K has a p-wave shape resonance at a collision energy of roughly 280 μK . At temperatures well below the resonant energy (less than 30 μK), a fit to σ_p vs T gives $\sigma_p \propto T^{2.0 \pm 0.3}$. Thus, we have directly observed the expected threshold behavior $\sigma_p \propto E^2$. In contrast, σ_s exhibits little temperature dependence. With these very different temperature dependencies, the collision rate changes by over two orders of magnitude at our lowest temperatures depending on the spin mixture of the fermionic atom gas.

To explore this effect further we measure the thermalization rate vs spin polarization at 9 μK (see Fig. 3). We control the relative populations of $|9/2, 9/2 \rangle$ and $|9/2, 7/2 \rangle$ atoms in a two-component cloud with a microwave field that drives transitions to untrapped spin states in the $F=7/2$ ground state manifold. The trap bias magnetic field breaks the degeneracy of the hyperfine ground-state splitting (1.286 GHz at zero field [20]) so that the different spin-states can be removed selectively (see Fig. 3 inset). For the data shown in Fig. 3 the fraction of atoms in the $|9/2, 9/2 \rangle$ state $f_{m_F=9/2} \equiv \frac{N_{m_F=9/2}}{N_{m_F=9/2} + N_{m_F=7/2}}$, was varied smoothly from 70 to 100% by varying the power of an applied microwave field (frequency swept) that removes a portion of the $|9/2, 7/2 \rangle$ atoms.

The thermalization of mixed spin-state samples depends on both s-wave and p-wave collisions. The data in Fig. 3 can be fit to a simple model given by:

$$1/\tau = n_{1,2} \left(\frac{2}{\alpha_s} \sigma_s + \frac{2}{\alpha_p} \frac{\sigma_p}{2} \right) v + (n_{1,1} + n_{2,2}) \frac{2}{\alpha_p} \sigma_p v,$$

where $n_{i,j}$ is the density-weighted density between two species given by $n_{i,j} = \frac{1}{N_1+N_2} \int n_i(r)n_j(r)d^3r$ and the subscripts 1 and 2 stand for the two relevant spin states. Since the magnetic moments of the $|9/2, 9/2 \rangle$ and $|9/2, 7/2 \rangle$ atoms are only slightly different we make the simplifying assumption that these states have identical spatial profiles in the trap. A fit using the above model with σ_s and the ratio σ_p/σ_s as free parameters shows good agreement with the data in Fig. 3. In addition to demonstrating the type of control over collision rates that is available in a trapped gas of fermionic atoms, this measurement of σ_p/σ_s at low temperature provides a sensitive constraint on the triplet scattering length. The s-wave cross-sections shown in Fig. 2 were extracted using the above equation, however at these low temperatures σ_p is relatively small and the measured thermalization rates are due primarily to s-wave interactions.

To compute the scattering cross sections for comparison with these data, we first identify singlet and triplet potassium potentials [21] that have been determined spectroscopically. At large interatomic separation R these potentials are matched smoothly to the long-range form of Marinescu *et al.* [22]. We add an additional correction to these potentials' inner walls [11], enabling us to tune the scattering lengths over their entire ranges $-\infty < a < \infty$. We set the singlet scattering length's value at $a_s = 104a_0$ [11] where a_0 is the Bohr radius, but leave the triplet scattering length a_t as a free parameter to be determined by the experiment. We note that the present experiment is relatively insensitive to the value of a_s since even the $|9/2, 9/2 \rangle + |9/2, 7/2 \rangle$ process is strongly triplet-dominated and no singlet resonance occurs near threshold; indeed, varying a_s over its range of uncertainty, $101 < a_s < 107$ [11], does not change the fit.

After computing cross sections as a function of collision energy, we determine temperature-dependent cross sections by computing a thermal average over collision events, weighted by the collision energy. Using this type of thermal averaging to account for a temperature-dependent cross section is supported by Monte Carlo studies [19]. To make a fit to the data, we compute χ^2 while floating both a_t and a multiplicative factor ϵ which scales simultaneously the computed $\sigma_s(T)$ and $\sigma_p(T)$. This factor is required to accommodate a $\pm 50\%$ systematic uncertainty in the experimental determination of absolute cross sections (primarily from N). Our global best fit occurs for $a_t = 157 \pm 20a_0$ and $\epsilon = 1.6$, with a reduced χ^2 of 3.8; the corresponding cross sections are plotted as lines in Fig. 2. The uncertainty in a_t reflects a doubling of the fit χ^2 and includes a $\sim 2a_0$ uncertainty arising from varying C_6 over its range $3600 < C_6 < 4000$ a.u. [22]. Our nominal potential gives a p-wave shape resonance at $\sim 280\mu\text{K}$ in collision energy, with an asymmetric lineshape whose FWHM is $\sim 400\mu\text{K}$.

The relatively small uncertainty on the value of a_t is attributable to the fact that we can simultaneously fit

s-wave and p-wave collision data having little relative uncertainty. The value of a_t for ^{40}K determined here does not agree well with reference [10], highlighting the importance of low temperature data in determining accurate potentials. Our measurement is however in good agreement with the value $a_t = 194_{-42}^{+172}$ obtained recently from an analysis of photoassociation spectroscopy of ^{39}K [11]. This agreement between two fundamentally different experiments is very encouraging, and suggests that the potassium scattering lengths are now fairly well determined [23]. Using our new value, we have tabulated in Table 1 the resulting triplet scattering lengths for collisions between the different potassium isotopes.

One of the important applications of these thermalization rate measurements is in determining the feasibility of various evaporative cooling strategies for this fermionic atom gas. The large p-wave cross section makes evaporation of a spin-polarized sample possible, but only at $T \gtrsim 20\mu\text{K}$. To reach lower temperatures, which is likely to be necessary for producing quantum degenerate samples, evaporation of a mixed spin-state sample should work well given the suitably large s-wave elastic collision cross section.

Indeed, for the data presented in this letter we vary the temperature of the sample through forced evaporation. To facilitate evaporative cooling, we increase the collision rate by ramping to a $\nu_r = 133 \pm 5$ Hz trap. Evaporation then proceeds using a mixed spin state sample and applying a microwave field to remove selectively the most energetic atoms (in both spin states). With these initial attempts at evaporatively cooling of ^{40}K we can lower the sample temperature from $100\mu\text{K}$ to $5\mu\text{K}$. We see runaway evaporation, where the collision rate in the gas increases as the temperature decreases. While the samples discussed in this work are still far from quantum degeneracy, this initial success and our measurement of a large s-wave elastic collision cross section bode well for future progress toward this goal.

This work is supported by the National Institute of Standards and Technology and the National Science Foundation. The authors would like to express their appreciation for useful discussions with C. Wieman and E. Cornell.

-
- * Quantum Physics Division, National Institute of Standards and Technology
[1] M.H. Anderson *et al.*, Science **269**, 198 (1995); K.B. Davis *et al.*, Phys. Rev. Lett. **75**, 3969 (1995); C.C. Bradley, C.A. Sackett, and R.G. Hulet, Phys. Rev. Lett. **78**, 985 (1997).
[2] J.M.K.V.A. Koelman *et al.*, Phys. Rev. Lett. **59**, 676 (1987).

- [3] A. Imamoglu and L. You, Phys. Rev. A **50** 2642 (1994); J. Javanainen and J. Ruostekoski, Phys. Rev. A **52** 3033 (1995); T. Busch *et al.*, Europhys. Lett. **44**, 1 (1998); B. DeMarco and D.S. Jin, Phys. Rev. A **58**, R4267 (1998).
- [4] A.J. Leggett, J. Phys. C (Paris) **7**, 19 (1980); H.T.C. Stoof *et al.*, Phys. Rev. Lett. **76**, 10 (1996); M.A. Baranov, Y. Kagan, and M.Y. Kagan, JETP Lett. **64** (1996); A.G.W. Modawi and A.J. Leggett, J. Low Temp. Phys. **109**, 625 (1998).
- [5] W.C. Stwalley, Phys. Rev. Lett. **37**, 1628 (1976); E. Tiesinga, B.J. Verhaar, and H. Stoof, Phys. Rev. A **47**, 4114 (1993).
- [6] H.F. Hess *et al.*, Phys. Rev. Lett. **59**, 672 (1987).
- [7] M. Marinescu and L. You, quant-ph/9810046.
- [8] C.J. Myatt *et al.*, Phys. Rev. Lett. **78**, 586 (1997).
- [9] H.M.J.M. Boesten *et al.*, Phys. Rev. A **54**, R3726 (1996).
- [10] R. Côté *et al.*, Phys. Rev. A **57**, R4118 (1998).
- [11] J.P. Burke *et al.*, submitted to Phys. Rev. A.
- [12] C. J. Myatt *et al.*, Opt. Lett. **21**, 290 (1996).
- [13] We use SDL power amplifier part SDL-8630-E; SDL is a trade name used for identification purposes only and does not constitute an endorsement by the authors or their institutions.
- [14] K.L. Corwin *et al.*, App. Optics **37**, 3295 (1998).
- [15] B. DeMarco, H. Rohner, and D.S. Jin, Rev. Sci. Instrum, in press.
- [16] R. Williamson III, PhD thesis, University of Wisconsin - Madison (1997); F. S. Cataliotti *et al.*, Phys. Rev. A **57**, 1136 (1998).
- [17] M. -O. Mewes *et al.*, Phys. Rev. Lett., **77**, 416 (1996).
- [18] C.R. Monroe *et al.*, Phys. Rev. Lett. **70**, 414 (1993).
- [19] For more details see M. Holland, unpublished.
- [20] E. Arimondo, M. Inguscio, and P. Violino, Rev. Mod. Phys. **49**, 31 (1977).
- [21] C. Amiot, J. Mol. Spect. **147**, 370 (1991); L. Li *et al.*, J. Chem. Phys. **93**, 8452 (1990); G. Zhao *et al.*, *Ibid.* **105** 7976 (1996).
- [22] M. Marinescu, H.R. Sadeghpour, and A. Dalgarno, Phys. Rev. A **49**, 982 (1994).
- [23] The result of Ref. [11] is somewhat sensitive to the value of C_6 , and is in better agreement with the present result for $C_6 = 4000$ a.u.

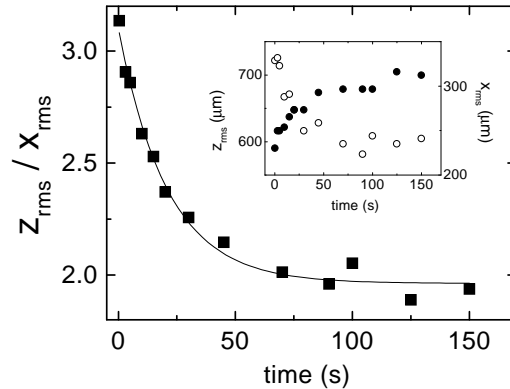


FIG. 1. Example of thermalization data. The inset shows the axial size, z_{rms} (\bullet), and the radial size, x_{rms} (\circ), imaged after 2.7 ms of free expansion, relaxing as the trapped atoms rethermalize via elastic collisions. At time=0 the cloud is taken out of equilibrium by changing ν_r from 133 to 44Hz. A fit (line) to the aspect ratio vs time is used to extract the relaxation rate.

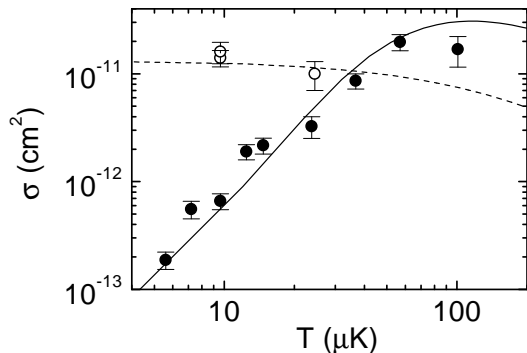


FIG. 2. Elastic cross sections vs. temperature. The s-wave cross section (\circ), measured using a mixture of spin states, shows little temperature dependence. However, the p-wave cross section (\bullet), measured using spin-polarized atoms, exhibits the expected threshold behavior and is seen to vary by over two orders of magnitude. The lines are a fit to the data, as described in the text, yielding $a_t = 157 \pm 20a_0$.

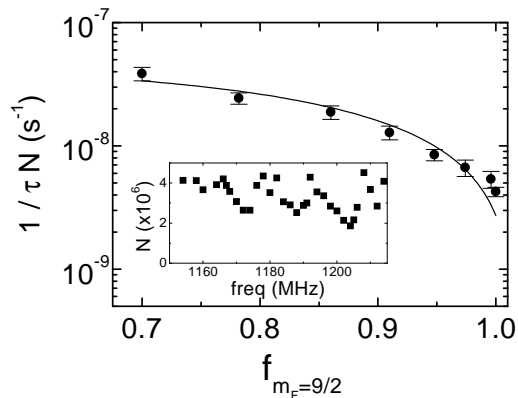


FIG. 3. Dependence of σ on spin composition at $T = 9\mu K$. A quantity proportional to σ , $1/\tau N$, is measured as a function of the fraction of atoms in one of two trapped Zeeman spin states, $f_{m_F=9/2}$. The inset shows the number of atoms remaining after application of microwaves at the indicated frequency. The three features correspond to removal of trapped atoms in particular spin states and can be used to measure or control the spin composition of the atom gas.

TABLE I. Triplet scattering lengths a_t in Bohr radii for collisions between potassium isotopes.

Isotopes	Nominal a_t	Range
40 + 40	157	$136 < a_t < 176$
39 + 39	-44	$-80 < a_t < -28$
41 + 41	57	$49 < a_t < 62$
39 + 40	3600	$a_t > 500$ or $a_t < -900$
39 + 41	164	$140 < a_t < 185$
40 + 41	93	$83 < a_t < 99$